



Dynamic Response of Twin Circular Unlined Tunnels Subjected to Blasting P Waves

Shiwei Lu^{1,2,3}, Yingkang Yao^{1,2*}, Yongsheng Jia^{1,2}, Jinshan Sun^{1,2}, Ling Ji⁴ and Zhen Zhang^{1,2}

¹State Key Laboratory of Precision Blasting, Jiangnan University, Wuhan, China, ²Hubei Key Laboratory of Blasting Engineering, Jiangnan University, Wuhan, China, ³School of Urban Construction, Yangtze University, Jingzhou, China, ⁴Faculty of Engineering, China University of Geosciences, Wuhan, China

The dynamic response of twin circular unlined tunnels is studied by indirect boundary integral equation method (IBIEM). The twin tunnels are assumed to lie in an unbounded elastic space subjected to blasting P waves. The influence of incident angle on the distribution of DSCF around the twin tunnels is analyzed. Besides, the influences of normalized wave number αa and normalized distance d^* (ratio of spacing distance to tunnel radius) on the reference DSCF, that is, the peak DSCF for different incident angles with an assurance rate of 95%, are discussed. Results show that 1) the IBIEM is a high-precision method analyzing the DSCF around twin circular unlined tunnels induced by blasting P waves; 2) the incident angle θ_0 , αa , and d^* all have significant influences on the distribution of DSCF; 3) for a constant d^* , the peak DSCF around the right tunnel is slightly greater than the left one; 4) the reference DSCF decreases exponentially with the increasing of αa or d^* , and the corresponding fitting functions are proposed.

Keywords: dynamic response, blasting wave, twin circular tunnel, dynamic stress concentration factor, indirect boundary integral equation method

INTRODUCTION

In recent years, underground tunnels have been widely developed due to transportation problems induced by the dramatic growth of population (Li et al., 2017; Zhang et al., 2021). In many populous cities, twin tunnels are increasingly constructed to improve transportation capacity (Alielahi and Adampira, 2016). When the drilling and blasting method is adopted, blasting waves will impose a potential danger on the adjacent existing tunnels (Xia et al., 2013; Zhou et al., 2016; Dang et al., 2018; Xue et al., 2019; Peng et al., 2021). Evaluating the dynamic response and proposing a safety criterion of the existing tunnels subjected to blasting waves are of the utmost importance.

In the past years, extensive studies have been carried out in evaluating the dynamic response of underground tunnels caused by incident waves. These studies mainly focus on the dynamic response of the rock or the lining of a single tunnel. Yi et al. (2008) studied the dynamic response of an arch-with-vertical-wall lining, and concluded that the incidence angle of incident waves has a significant influence on the critical vibration velocity. Furthermore, Yi et al. (2016) discussed the dynamic response of a circular lined tunnel with an imperfectly bonded interface under plane P waves, and found that the interface stiffness has a great influence on the distribution of dynamic stress concentration factors (DSCF) of the tunnel. Pao and Mow (1973) investigated the dynamic stress concentration of lined and unlined circular tunnels subjected to plane P and S waves numerically. Lu et al. (2019a), Lu et al. (2019b), and Lu et al. (2021) studied the DSCF and peak particle velocity of a circular tunnel subjected to cylindrical P waves theoretically. Wang et al.

OPEN ACCESS

Edited by:

Xiaodong Fu,
Institute of Rock and Soil Mechanics
(CAS), China

Reviewed by:

Yaxiong Peng,
Hunan University of Science and
Technology, China
Su Hong,
Anhui University of Science and
Technology, China

*Correspondence:

Yingkang Yao
shanxiyao@jhu.edu.cn

Specialty section:

This article was submitted to
Geohazards and Georisks,
a section of the journal
Frontiers in Earth Science

Received: 11 May 2022

Accepted: 27 May 2022

Published: 07 July 2022

Citation:

Lu S, Yao Y, Jia Y, Sun J, Ji L and
Zhang Z (2022) Dynamic Response of
Twin Circular Unlined Tunnels
Subjected to Blasting P Waves.
Front. Earth Sci. 10:941070.
doi: 10.3389/feart.2022.941070

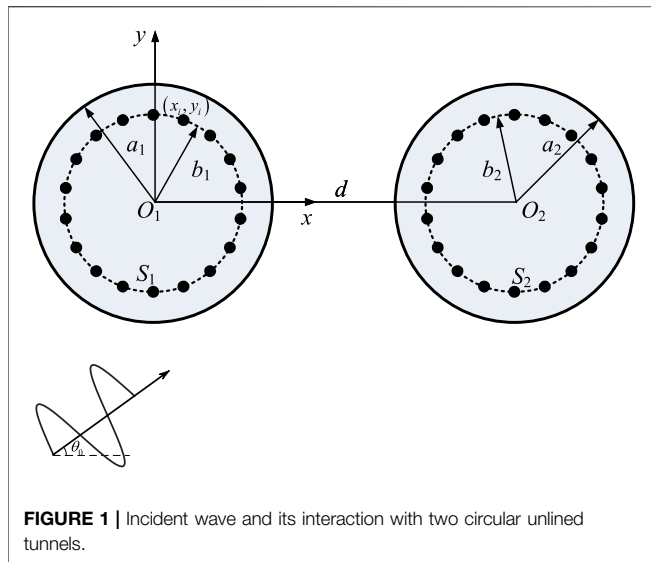


FIGURE 1 | Incident wave and its interaction with two circular unlined tunnels.

(2014) studied the dynamic responses of the tunnel at various depths in double-layer rocks by finite element method. Li et al. (2018) firstly proposed the theoretical formula to evaluate the DSCF around a circular opening subjected to blasting wave and studied the dynamic response of deep-buried tunnels under triangular blasting loads. Liu et al. (2011) and Chen et al. (2012) discussed the dynamic response of a rock tunnel subjected to harmonic P, S, and R waves by numerical simulation method. Xu et al. (2014) investigated the effects of incident frequency, incident angle, and rock conditions on a circular lining tunnel subjected to incident plane P waves. Zhang et al. (2022) explored the stresses and vibrations of a single circular tunnel under the incidence of cylindrical P waves and proposed the PPV criterion. Qiu et al. (2022) studied the blasting dynamic behavior of deep buried tunnels and discussed their safety. Zlatanović et al. (2021) and Yuan et al. (2020) explored the influence of new structures on the dynamic responses of existing tunnels subjected to different incident waves. Although the study on different factors influencing dynamic response of underground tunnels subjected to incident waves has made

great progress, the quantitative relationship between different factors and dynamic response of tunnels subjected to incident waves is very limited.

In this article, the dynamic response of twin circular unlined tunnels subjected to blasting P waves is studied by indirect boundary integral equation method (IBIEM). The influence of the incident angle on DSCF of the twin tunnels is analyzed. Furthermore, the influences of normalized wave number and normalized distance (ratio of spacing distance to tunnel radius) on the reference DSCF, that is, the peak DSCF for different incident angles with an assurance rate of 95%, are discussed. The fitting functions determining the reference DSCF are proposed.

INTERACTION OF BLASTING P WAVES AND TWIN CIRCULAR UNLINED TUNNELS

Assume two circular unlined tunnels with a distance d lie in an unbounded space, centering at O_1 and O_2 , respectively. The radii are denoted by a_1 on the left side and a_2 on the right side. A right-handed Cartesian coordinate system O_1xy is established, as shown in **Figure 1**. The virtual sources are represented by S_1 and S_2 with less radii b_1 and b_2 to simulate the outgoing waves and avoid singularity on the tunnel boundaries. The displacement potential function of incident P wave can be expressed as:

$$\varphi^{(i)} = \varphi_0 e^{i\alpha(x \cos \theta_0 + y \sin \theta_0) - i\omega t} \tag{1}$$

where φ_0 is the amplitude of incident wave, α is the wave number of P waves and $\alpha = \omega/c_p$, ω is the circular frequency of incident wave, c_p is the phase velocity of incident wave, θ_0 is the incident angle, and i is the unit of complex number.

Let φ denote the linear sum of the potentials of the incident and diffracted P waves, ψ denote the linear sum of the potential of the incident and diffracted S wave, then

$$\begin{aligned} \varphi &= \varphi^{(i)} + \sum_{i=1}^M \varphi_i^{(d)} + \sum_{i=M+1}^{M+N} \varphi_i^{(d)} \\ \psi &= \sum_{i=1}^M \psi_i^{(d)} + \sum_{i=M+1}^{M+N} \psi_i^{(d)} \end{aligned} \tag{2}$$

TABLE 1 | Relative errors for different numbers of source and observation points.

αa	Number of Source Points	Number of Observation Points	Err				
			$\theta_0 = 0^\circ$	$\theta_0 = 30^\circ$	$\theta_0 = 45^\circ$	$\theta_0 = 60^\circ$	$\theta_0 = 90^\circ$
0.1	10	20	8.958×10^{-1}	1.260	3.097×10^{-1}	5.360×10^{-1}	6.252×10^{-1}
	20	30	4.692×10^{-1}	6.720×10^{-1}	8.279×10^{-2}	1.867×10^{-1}	2.347×10^{-1}
	30	50	2.937×10^{-1}	3.730×10^{-1}	1.460×10^{-1}	2.114×10^{-1}	2.052×10^{-1}
	40	60	1.020×10^{-1}	1.318×10^{-1}	8.113×10^{-2}	5.402×10^{-2}	3.604×10^{-2}
	60	80	8.896×10^{-5}	1.014×10^{-4}	4.142×10^{-5}	3.550×10^{-5}	1.701×10^{-5}
	80	100	2.142×10^{-8}	2.433×10^{-8}	9.958×10^{-9}	8.544×10^{-9}	4.068×10^{-9}
2	10	20	3.306×10^{-1}	3.381×10^{-1}	4.959×10^{-1}	4.245×10^{-1}	5.203×10^{-1}
	20	30	4.255×10^{-2}	2.517×10^{-2}	2.323×10^{-2}	4.000×10^{-3}	2.544×10^{-2}
	30	50	2.432×10^{-2}	3.205×10^{-2}	3.644×10^{-2}	5.567×10^{-2}	3.085×10^{-2}
	40	60	3.872×10^{-4}	8.382×10^{-4}	2.205×10^{-3}	1.270×10^{-2}	4.009×10^{-3}
	60	80	3.627×10^{-5}	9.693×10^{-5}	5.418×10^{-4}	1.542×10^{-3}	7.193×10^{-4}
	80	100	5.410×10^{-8}	3.082×10^{-7}	9.357×10^{-7}	2.328×10^{-6}	1.236×10^{-6}

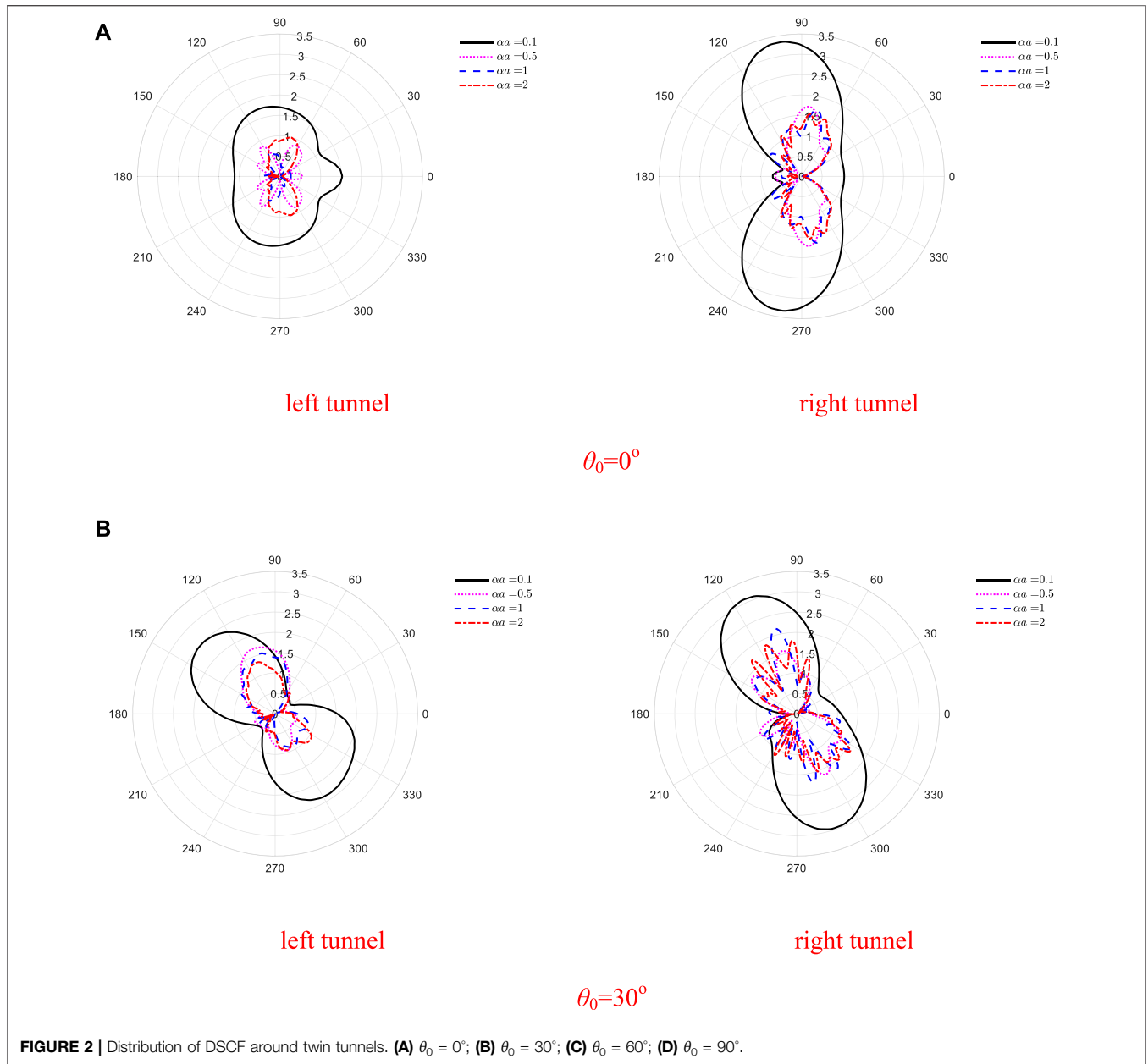


FIGURE 2 | Distribution of DSCF around twin tunnels. (A) $\theta_0 = 0^\circ$; (B) $\theta_0 = 30^\circ$; (C) $\theta_0 = 60^\circ$; (D) $\theta_0 = 90^\circ$.

where M and N are the numbers of virtual sources in the left and right tunnels, $\varphi_i^{(d)}$ and $\psi_i^{(d)}$ are the potential functions of diffracted P and SV waves generated by the i -th virtual source.

The diffracted waves generated by the i -th virtual source can be expressed in terms of 0-th Hankel functions as:

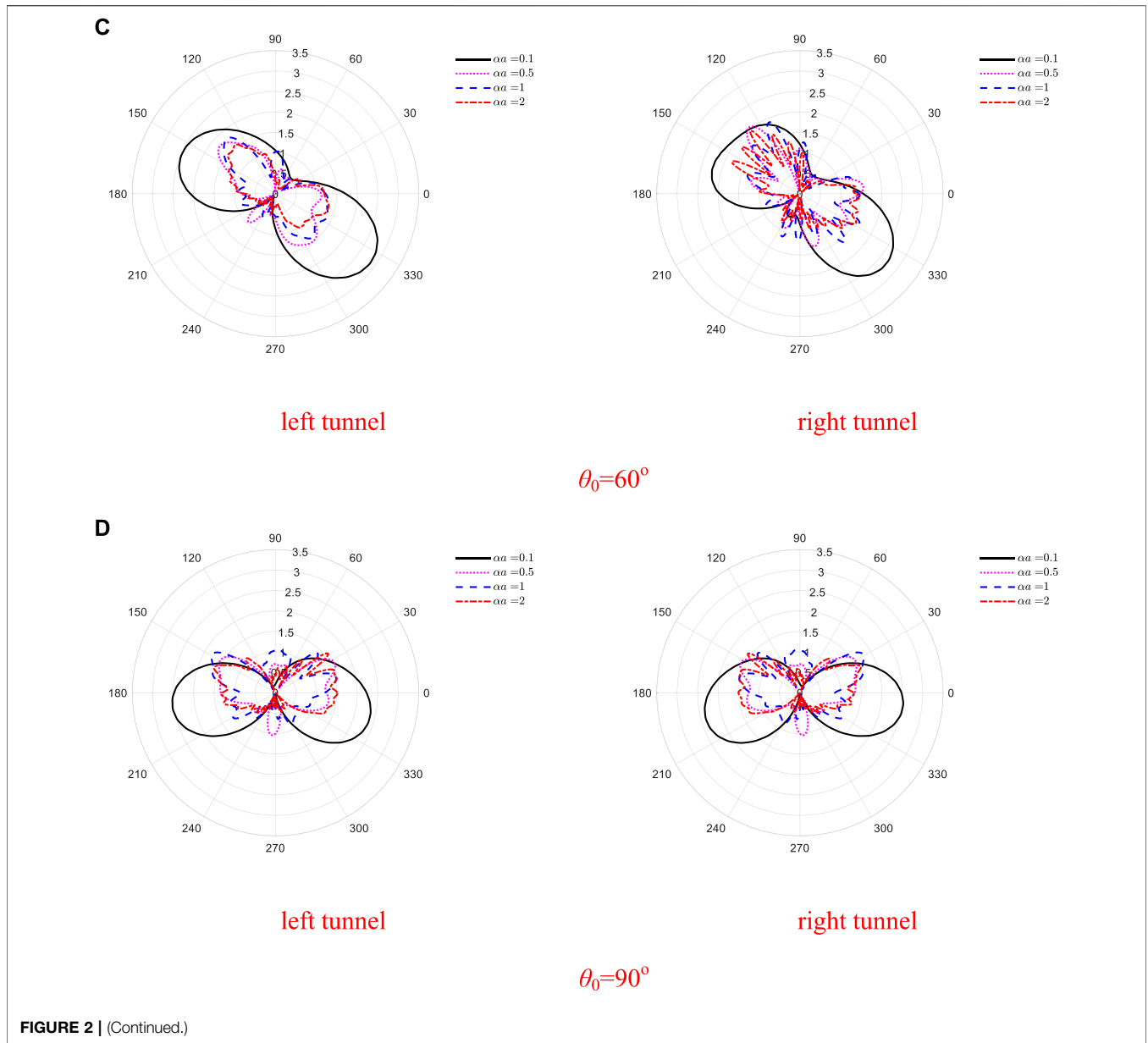
$$\varphi_i^{(d)} = A_i H_0^{(1)}(\alpha R_i) e^{-i\omega t} \tag{3}$$

$$\psi_i^{(d)} = B_i H_0^{(1)}(\beta R_i) e^{-i\omega t} \tag{4}$$

where R_i is the distance between an arbitrary point in the surrounding rock and the i -th virtual source, defined by $R_i = \sqrt{(x - x_i)^2 + (y - y_i)^2}$, β is the wave number of S waves.

According to the relations between stress and displacement, the stress can be expressed as:

$$\begin{cases} u_x = \frac{\partial \varphi}{\partial x} + \frac{\partial \psi}{\partial y} \\ u_y = \frac{\partial \varphi}{\partial y} - \frac{\partial \psi}{\partial x} \\ \frac{\sigma_{xx}}{\mu} = \left(\frac{\beta^2}{\alpha^2} - 2\right) \nabla^2 \varphi + 2\left(\frac{\partial^2 \varphi}{\partial x^2} + \frac{\partial^2 \psi}{\partial x \partial y}\right) \\ \frac{\sigma_{yy}}{\mu} = \left(\frac{\beta^2}{\alpha^2} - 2\right) \nabla^2 \varphi + 2\left(\frac{\partial^2 \varphi}{\partial y^2} - \frac{\partial^2 \psi}{\partial x \partial y}\right) \\ \frac{\sigma_{xy}}{\mu} = 2\left(\frac{\partial^2 \varphi}{\partial x \partial y} + \frac{\partial^2 \psi}{\partial y^2} - \frac{\partial^2 \psi}{\partial x^2}\right) \end{cases} \tag{5}$$



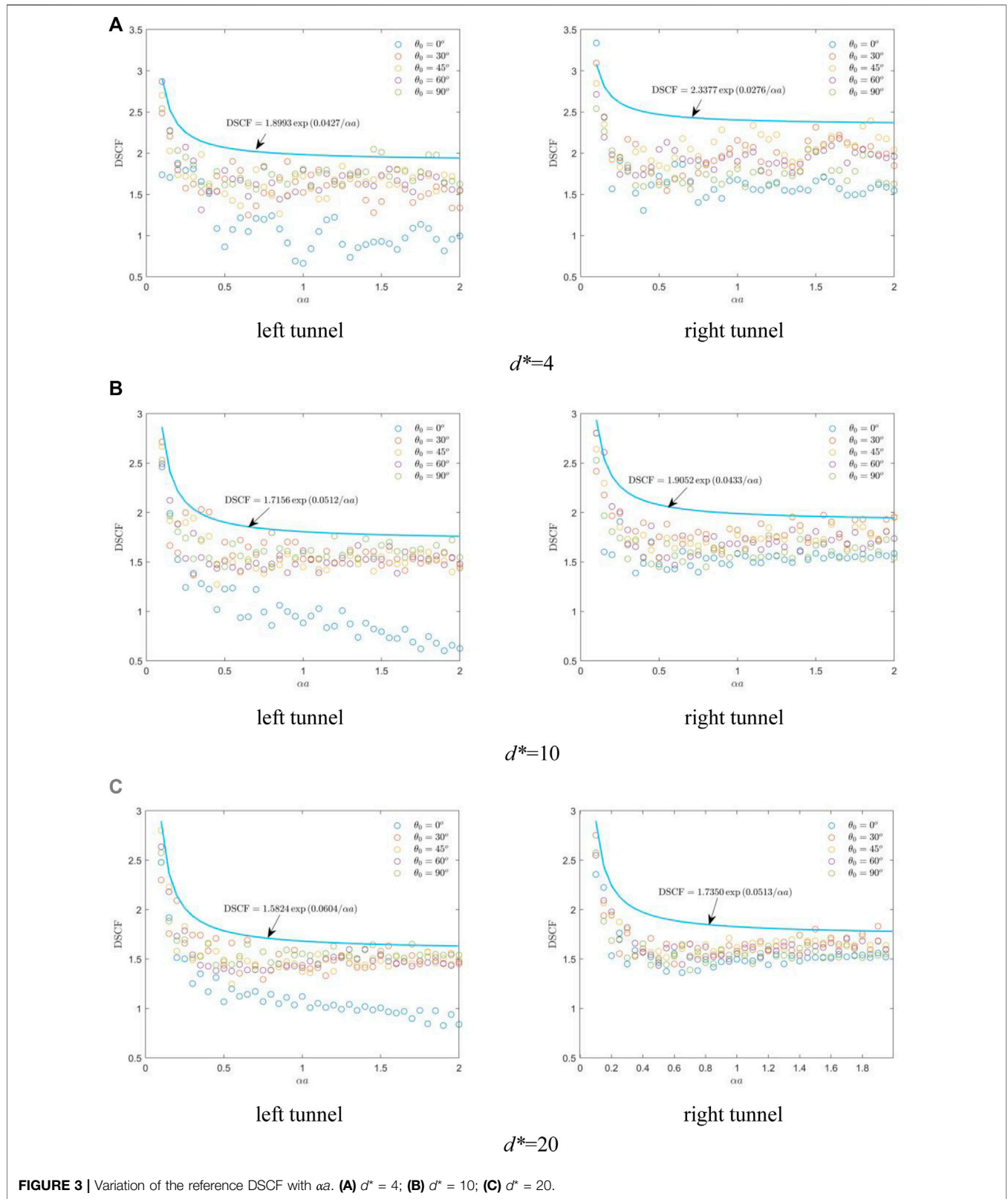
Then substituting Eqs 1–4 into Eq. 5, the displacements and stresses can be written as follows:

$$u_x = i\alpha\varphi_0 \cos \theta_0 e^{i\alpha(x \cos \theta_0 + y \sin \theta_0)} - \sum_{i=1}^{M+N} \frac{\alpha A_i (x - x_i) H_1^{(1)}(\alpha R_i)}{R_i} - \sum_{i=1}^{M+N} \frac{\beta B_i (y - y_i) H_1^{(1)}(\beta R_i)}{R_i} \quad (6a)$$

$$u_y = i\alpha\varphi_0 \sin \theta_0 e^{i\alpha(x \cos \theta_0 + y \sin \theta_0)} - \sum_{i=1}^{M+N} \frac{\alpha A_i (y - y_i) H_1^{(1)}(\alpha R_i)}{R_i} + \sum_{i=1}^{M+N} \frac{\beta B_i (x - x_i) H_1^{(1)}(\beta R_i)}{R_i} \quad (6b)$$

$$\frac{\sigma_{xx}}{\mu} = (2\alpha^2 \sin^2 \theta_0 - \beta^2) \varphi_0 e^{i\alpha(x \cos \theta_0 + y \sin \theta_0)} + \sum_{i=1}^{M+N} A_i \left\{ \left[2\alpha^2 \frac{(y - y_i)^2}{R_i^2} - \beta^2 \right] H_0^{(1)}(\alpha R_i) + 2\alpha \left[\frac{2(x - x_i)^2}{R_i^3} - \frac{1}{R_i} \right] H_1^{(1)}(\alpha R_i) \right\} + \sum_{i=1}^{M+N} B_i \left\{ 4\beta \frac{(x - x_i)(y - y_i)}{R_i^3} H_1^{(1)}(\beta R_i) - 2\beta^2 \frac{(x - x_i)(y - y_i)}{R_i^2} H_0^{(1)}(\beta R_i) \right\} \quad (6c)$$

$$\frac{\sigma_{yy}}{\mu} = (2\alpha^2 \cos^2 \theta_0 - \beta^2) \varphi_0 e^{i\alpha(x \cos \theta_0 + y \sin \theta_0)} + \sum_{i=1}^{M+N} A_i \left\{ \left[2\alpha^2 \frac{(x - x_i)^2}{R_i^2} - \beta^2 \right] H_0^{(1)}(\alpha R_i) + 2\alpha \left[\frac{2(y - y_i)^2}{R_i^3} - \frac{1}{R_i} \right] H_1^{(1)}(\alpha R_i) \right\} - \sum_{i=1}^{M+N} B_i \left\{ 4\beta \frac{(x - x_i)(y - y_i)}{R_i^3} H_1^{(1)}(\beta R_i) - 2\beta^2 \frac{(x - x_i)(y - y_i)}{R_i^2} H_0^{(1)}(\beta R_i) \right\} \quad (6d)$$



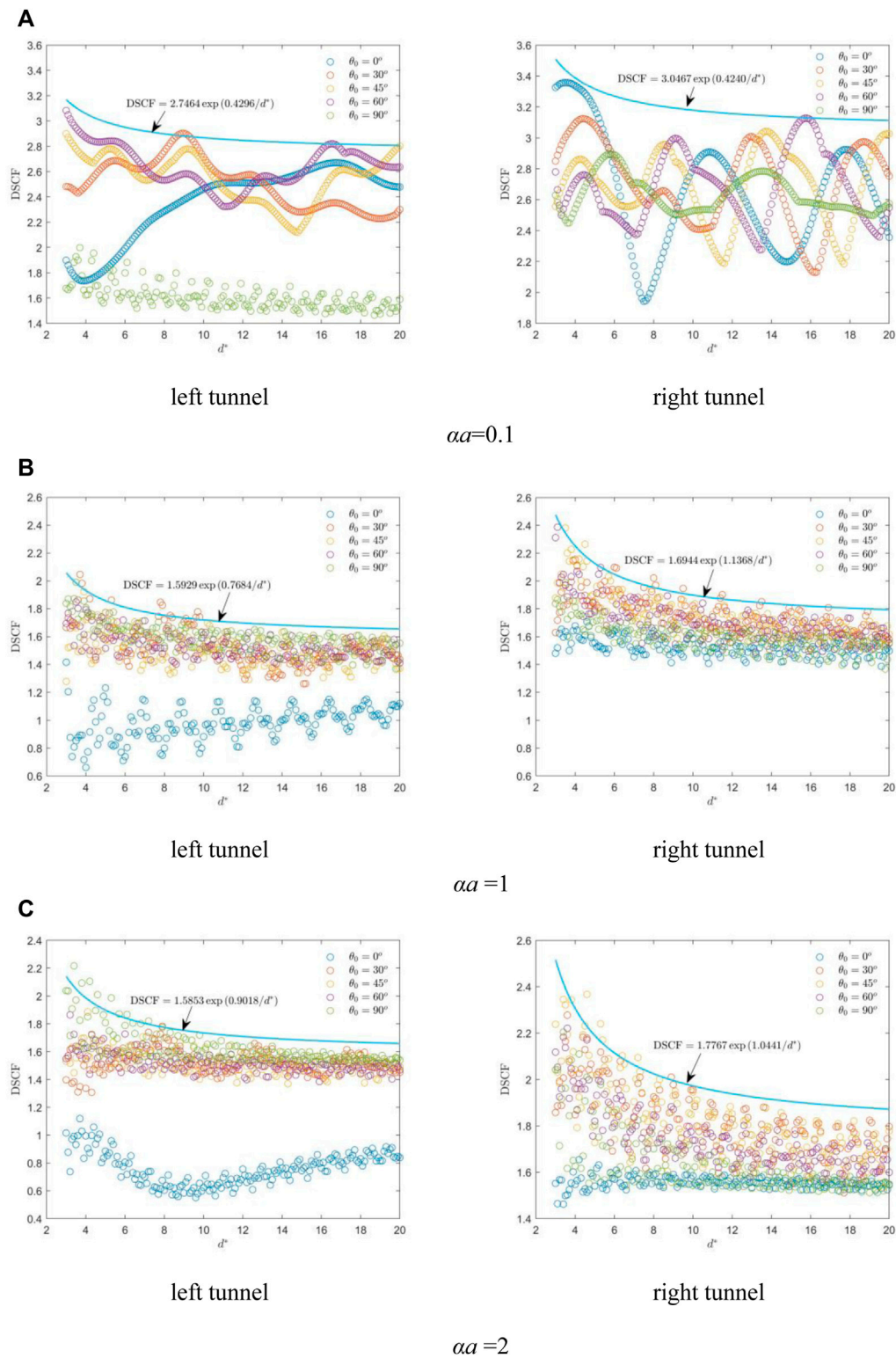


FIGURE 4 | Variation of DSCF with d^* . **(A)** $aa = 0.1$; **(B)** $aa = 1$; **(C)** $aa = 2$.

TABLE 2 | Summation of fitting functions with respect to αa .

d^*	Fitting Functions	
	Left Tunnel	Right Tunnel
4	DSCF = 1.8993 exp(0.0427/ αa)	DSCF = 2.3377 exp(0.0276/ αa)
10	DSCF = 1.7156 exp(0.0512/ αa)	DSCF = 1.9052 exp(0.0433/ αa)
20	DSCF = 1.5824 exp(0.0604/ αa)	DSCF = 1.7350 exp(0.0513/ αa)

TABLE 3 | Summation of fitting functions with respect to d^* .

αa	Fitting Functions	
	Left Tunnel	Right Tunnel
0.1	DSCF = 2.7464 exp(0.4296/ d^*)	DSCF = 3.0467 exp(0.4240/ d^*)
1	DSCF = 1.5929 exp(0.7684/ d^*)	DSCF = 1.6944 exp(1.1368/ d^*)
2	DSCF = 1.5853 exp(0.9018/ d^*)	DSCF = 1.7767 exp(1.0441/ d^*)

$$\frac{\sigma_{xy}}{\mu} = -\alpha^2 \sin 2\theta_0 \varphi_0 e^{i\alpha(x \cos \theta_0 + y \sin \theta_0)} + \sum_{i=1}^{M+N} A_i \left\{ 4\alpha \frac{(x-x_i)(y-y_i)}{R_i^3} H_1^{(1)}(\alpha R_i) - 2\alpha^2 \frac{(x-x_i)(y-y_i)}{R_i^2} H_0^{(1)}(\alpha R_i) \right\} - \sum_{i=1}^{M+N} B_i \left\{ 2\beta \frac{(x-x_i)^2 - (y-y_i)^2}{R_i^3} H_1^{(1)}(\beta R_i) - \beta^2 \frac{(x-x_i)^2 - (y-y_i)^2}{R_i^2} H_0^{(1)}(\beta R_i) \right\} \quad (6e)$$

The stress components in Cartesian coordinate system can be transformed to those in polar coordinate system by the following equations.

$$\begin{cases} u_r = u_x \cos \theta + u_y \sin \theta \\ u_\theta = -u_x \sin \theta + u_y \cos \theta \\ \sigma_{rr} = \sigma_{xx} \cos^2 \theta + \sigma_{yy} \sin^2 \theta + \sigma_{xy} \sin 2\theta \\ \sigma_{\theta\theta} = \sigma_{xx} \sin^2 \theta + \sigma_{yy} \cos^2 \theta - \sigma_{xy} \sin 2\theta \\ \sigma_{r\theta} = (\sigma_{yy} - \sigma_{xx}) \sin \theta \cos \theta + \sigma_{xy} \cos 2\theta \end{cases} \quad (7)$$

The traction-free boundary conditions are given by

$$\sigma_{rr} = \sigma_{r\theta} = 0 \quad \text{for} \quad \begin{cases} x = a_1 \cos \theta \\ y = a_1 \sin \theta \end{cases} \quad \text{and} \quad \begin{cases} x = d + a_2 \cos \theta \\ y = a_2 \sin \theta \end{cases} \quad (8)$$

Substituting Eqs 6a–6e and 7 into Eq. 8, the boundary conditions can be rewritten in the matrix form.

$$HA = S \quad (9)$$

where H is the Green’s influence matrix, A is the undermined coefficients representing the source density, and S is the vector of stresses induced by the incident wave.

In general, Eq. 9 is overdetermined, and only the approximate solution can be obtained by the least square method.

$$A = [H'H]^{-1} H'S \quad (10)$$

The relative error is always determined as follows:

$$Err = |HA - S|/|S| \quad (11)$$

where $||$ is the Euclidean norm of a vector.

DSCF is an important parameter to evaluate structural stability (Fan et al., 2019; Ming et al., 2019; Jang et al., 2020; Li et al., 2020), which is defined as follows:

$$DSCF = \left| \frac{\sigma_{\theta\theta}}{\sigma_0} \right| \quad (12)$$

where σ_0 is the stress intensity of the incident wave in the direction of propagation, defined by $\sigma_0 = \mu \beta^2 \varphi_0$, μ is the shear modulus.

In order to get some general results, we need to define the following dimensionless parameter: the normalized distance as $d^* = d/a$, where a is the maximum of a_1 and a_2 . αa is another quite important index, generally called the dimensionless wave

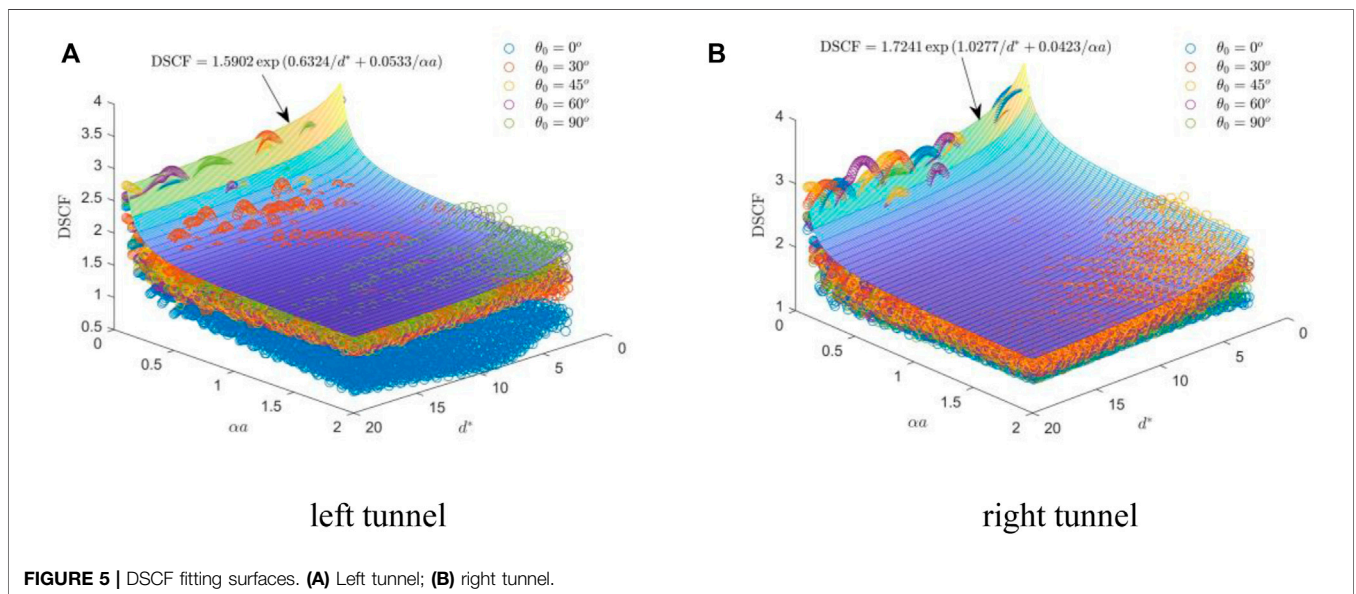


FIGURE 5 | DSCF fitting surfaces. (A) Left tunnel; (B) right tunnel.

number, which equals 2π times the ratio of a to the wave length of the incident wave.

ACCURACY ANALYSIS

In order to determine the calculation accuracy, we choose the case of $d^*=4$ for analysis. **Table 1** shows the relative errors determined by **Eq. 11** for different θ_0 when $\alpha a = 0.1$ and 2. The numbers of source points and observation points are generally different and the previous is less.

It is found that the relative error decreases with the increasing numbers of source and observation points. When the numbers of source and observation points equal to 60 and 80, the maximum relative errors are 1.014×10^{-4} for $\alpha a = 0.1$ and 1.542×10^{-3} for $\alpha a = 2$, which are sufficiently accurate. When the numbers of source and observation points equal to 80 and 100, the maximum relative errors are 2.433×10^{-8} for $\alpha a = 0.1$ and 2.328×10^{-6} for $\alpha a = 2$, which become far smaller. Therefore, we believe that 80 source points and 100 observation points are suitable in the following analysis.

RESULTS AND DISCUSSIONS

The distribution of DSCF around the twin tunnels under different αa and θ_0 is shown in **Figure 2**, where $d^* = 4$.

The DSCF of the tunnels is approximately symmetrically distributed about the incident direction for $\alpha a = 0.1$, and it becomes more complex with the increase of αa . It is obvious that the distribution of DSCF around the twin tunnels changes obviously with the variation of θ_0 . For the left tunnel, the peak DSCF around the left tunnel at $\theta_0 = 0^\circ$ is smaller than that at others for a fixed αa . For the right tunnel, the peak DSCF around the right tunnel occurs at $\theta_0 = 0^\circ$ for $\alpha a = 0.1$, while at others for $\alpha a = 0.5, 1$, and 2. This suggests that the incident angle θ_0 of blasting P waves has a significant influence on the distribution of DSCF.

For a fixed θ_0 , the peak DSCF at $\alpha a = 0.1$ is obviously greater than other cases, but the values at $\alpha a = 0.5, 1$, and 2 do not change apparently, which indicates that the peak DSCF decreases quickly at first, then varies slower and slower, eventually tends to a steady value.

Although the left tunnel is located at the incident side, the DSCF of the right tunnel is larger under the same αa , which may result from that the left tunnel deflects and focuses stress on, just like a convex lens.

According to the above analysis, the DSCF of tunnels changes with θ_0 . In a practical project, θ_0 may be unknown and the upper bound of DSCF for different θ_0 has a critical reference value for engineers. **Figure 3** and **Figure 4** show the variation of the reference DSCF (i.e., 95% of peak DSCF values are less than the given value) with αa and d^* , respectively.

It is found from **Figure 3** that the peak DSCF around the left tunnel is more discrete than the right tunnel and its decreasing

rate with αa for $\theta_0 = 0^\circ$ is obviously greater. The discreteness reduces with the increasing value of d^* . By using the least square method, we found the variation of the reference DSCF can be well fitted exponential functions. According to the fitting functions, the attenuation of peak DSCF around the left tunnel is faster than the right tunnel for a same d^* .

The summation of fitting functions in **Figure 3** is listed in **Table 2**.

It is observed from **Figure 4** that the peak DSCF for the left tunnel fluctuates obviously at $\alpha a = 0.1$, the variation tendency becomes clearer at $\alpha a = 1$ and 2. Besides, the smallest DSCF occurs at $\theta_0 = 90^\circ$ for $\alpha a = 0.1$ while at $\theta_0 = 0^\circ$ for $\alpha a = 1$ and 2. For the right tunnel, the peak DSCF shows a wave-like change at $\alpha a = 0.1$. When $\alpha a = 1$ and 2, the variation trends of DSCF with d^* are similar, the peak value of DSCF occurs at $\theta_0 = 30^\circ$ or 45° . Compared with the left tunnel, the distribution of peak DSCF of the right tunnel is more concentrated.

It is also found that the variation of the reference DSCF can be well fitted exponential functions. According to the fitting functions, the attenuation of peak DSCF around the right tunnel is faster for a constant αa while slower for a constant d^* compared with that around the left tunnel.

The summation of fitting functions in **Figure 4** is listed in **Table 3**.

Based on the above analysis, the attenuation of the reference DSCF with αa or d^* can be well expressed by exponential functions. Considering the joint impact of αa and d^* , the DSCF changing with both αa and d^* of the twin tunnels is shown in **Figure 5**.

The fitting surfaces for both tunnels are expressed in **Eq. 13**.

$$\text{DSCF} = \begin{cases} 1.5902 \exp(0.6324/d^* + 0.0533/\alpha a) & \text{for the left tunnel} \\ 1.7241 \exp(1.0277/d^* + 0.0423/\alpha a) & \text{for the right tunnel} \end{cases} \quad (13)$$

It is found that the fitting function can well reflect the previous results and αa has a greater influence on DSCF than d^* . **Eq. 13** can be proposed as the reference function and engineers can quickly obtain the critical value to prevent damage to such underground structures.

CONCLUSION

In this article, the dynamic response of twin circular unlined tunnels in an unbounded space subjected to blasting P waves is studied. According to the research results, the following conclusions can be obtained:

- (1) The DSCF around twin circular unlined tunnels subjected to blasting P waves is calculated by indirect boundary integral equation method, which is of high precision.
- (2) The incident angle θ_0 , normalized wave number αa , and normalized distance d^* all have a significant influence on the distribution of DSCF around the twin tunnels.

- (3) For a constant d^* , the peak DSCF around the right tunnel is slightly greater than the left one.
- (4) The reference DSCF decreases exponentially with the increase of $\alpha\alpha$ or d^* , and the corresponding fitting functions are proposed. Compared with d^* , the influence of $\alpha\alpha$ is more distinct.

DATA AVAILABILITY STATEMENT

The datasets presented in this study can be found in online repositories. The names of the repository/repositories and accession number(s) can be found in the article/Supplementary Material.

REFERENCES

- Alielahi, H., and Adampira, M. (2016). Effect of Twin-Parallel Tunnels on Seismic Ground Response Due to Vertically In-Plane Waves. *Int. J. Rock Mech. Min. Sci.* 85, 67–83. doi:10.1016/j.ijrmms.2016.03.010
- Chen, C.-H., Wang, T.-T., Jeng, F.-S., and Huang, T.-H. (2012). Mechanisms Causing Seismic Damage of Tunnels at Different Depths. *Tunn. Undergr. Space Technol.* 28 (1), 31–40. doi:10.1016/j.tust.2011.09.001
- Dang, V. K., Dias, D., Do, N. A., and Vo, T. H. (2018). Impact of Blasting at Tunnel Face on an Existing Adjacent Tunnel [J]. *Int. J. GEOMATE* 15 (47), 22–31. doi:10.21660/2018.47.04640
- Fan, Z., Zhang, J., and Xu, H. (2019). Theoretical Study of the Dynamic Response of a Circular Lined Tunnel with an Imperfect Interface Subjected to Incident SV-Waves. *Comput. Geotechnics* 110, 308–318. doi:10.1016/j.compgeo.2019.02.026
- Jang, P., Ri, Y., Ri, S., Pang, C., and Ok, C. (2020). Scattering of SH Wave by a Semi-Circle Inclusion Embedded in Bi-material Half Space Surface. *J. Mech.* 36 (4), 497–506. doi:10.1017/jmech.2019.72
- Li, S., Liu, B., Xu, X., Nie, L., Liu, Z., Song, J., et al. (2017). An Overview of Ahead Geological Prospecting in Tunneling. *Tunn. Undergr. Space Technol.* 63, 69–94. doi:10.1016/j.tust.2016.12.011
- Li, X., Li, C., Cao, W., and Tao, M. (2018). Dynamic Stress Concentration and Energy Evolution of Deep-Buried Tunnels under Blasting Loads. *Int. J. Rock Mech. Min. Sci.* 104, 131–146. doi:10.1016/j.ijrmms.2018.02.018
- Li, Z., Tao, M., Du, K., Cao, W., and Wu, C. (2020). Dynamic Stress State Around Shallow-Buried Cavity under Transient P Wave Loads in Different Conditions. *Tunn. Undergr. Space Technol.* 97, 103228. doi:10.1016/j.tust.2019.103228
- Liu, Z., Liang, J., and Zhang, H. (2011). Scattering of Rayleigh Wave by a Lined Tunnel in Elastic Half-Space [J]. *Chin. J. Rock Mech. Eng.* 30 (8), 1627–1637. (in Chinese).
- Lu, S., Zhou, C., Zhang, Z., Ji, L., and Jiang, N. (2021). Theoretical Study on Dynamic Responses of an Unlined Circular Tunnel Subjected to Blasting P-Waves. *J. Mech.* 37, 242–252. doi:10.1093/jom/ufaa029
- Lu, S., Zhou, C., Zhang, Z., and Jiang, N. (2019a). Dynamic Stress Concentration of Surrounding Rock of a Circular Tunnel Subjected to Blasting Cylindrical P-Waves. *Geotech. Geol. Eng.* 37, 2363–2371. doi:10.1007/s10706-018-00761-5
- Lu, S., Zhou, C., Zhang, Z., and Jiang, N. (2019b). Particle Velocity Response of Surrounding Rock of a Circular Tunnel Subjected to Cylindrical P-Waves. *Tunn. Undergr. Space Technol.* 83, 393–400. doi:10.1016/j.tust.2018.09.020
- Ming, T., Li, Z., Cao, W., Li, X., and Wu, C. (2019). Stress Redistribution of Dynamic Loading Incident with Arbitrary Waveform through a Circular Cavity[J]. *Int. J. Numer. Anal. Methods Geomechanics* 43 (6), 1279–1299. doi:10.3303/CET1655006
- Pao, Y. H., and Mow, C. C. (1973). *The Diffraction of Elastic Waves and Dynamic Stress Concentrations [M]*. New York: Crane, Russak & Company Inc.
- Peng, Y., Liu, G., Wu, L., Zuo, Q., Liu, Y., and Zhang, C. (2021). Comparative Study on Tunnel Blast-Induced Vibration for the Underground Cavern Group [J]. *Environ. Earth Sci.* 80 (2), 100–111. doi:10.1007/s12665-020-09362-z
- Qiu, J., Liu, K., and Li, X., (2022). Influence of Blasting Disturbance on Dynamic Response and Safety of Deep Tunnels [J]. *Geomechanics Geophys. Geo-Energy Geo-Resources* 8, 1–17. doi:10.1007/s40948-021-00308-8
- Wang, T.-T., Hsu, J.-T., Chen, C.-H., and Huang, T.-H. (2014). Response of a Tunnel in Double-Layer Rocks Subjected to Harmonic P- and S-Waves. *Int. J. Rock Mech. Min. Sci.* 70, 435–443. doi:10.1016/j.ijrmms.2014.06.002

AUTHOR CONTRIBUTIONS

Conceptualization: SL, YY; Methodology: SL and YJ; Formal analysis and investigation: JS, SL, and ZZ; Draft preparation: SL and LJ.

FUNDING

The study was sponsored by the Hubei Provincial Natural Science Foundation (Grant No. 2019CFB224), Hubei Provincial Department of Education (Grant No. Q20191308), and Open Research Fund of Hubei Key Laboratory of Blasting Engineering (Grant No. HKLBEF202011).

- Xia, X., Li, H. B., Li, J. C., Liu, B., and Yu, C. (2013). A Case Study on Rock Damage Prediction and Control Method for Underground Tunnels Subjected to Adjacent Excavation Blasting. *Tunn. Undergr. Space Technol.* 35, 1–7. doi:10.1016/j.tust.2012.11.010
- Xu, H., Li, T. B., Xu, J., and Wang, L. J. (2014). Dynamic Response of Underground Circular Lining Tunnels Subjected to Incident P Waves[J]. *Math. Problems Eng.* 2014, 297424. doi:10.1155/2014/297424
- Xue, F., Xia, C., Li, G., Jin, B., He, Y., and Fu, Y. (2019). Safety Threshold Determination for Blasting Vibration of the Lining in Existing Tunnels under Adjacent Tunnel Blasting. *Adv. Civ. Eng.* 2019 (3), 1–10. doi:10.1155/2019/8303420
- Yi, C., Lu, W., Zhang, J., and Zhang, A. P. (2008). Study on Critical Failure Vibration Velocity of Arch with Vertical Wall Lining Subjected to Blasting Vibration[J]. *Rock Soil Mech.* 29 (8), 2203–2208. (in Chinese). doi:10.3969/j.issn.1000-7598.2008.08.034
- Yi, C. P., Lu, W. b., Zhang, P., Johansson, D., and Nyberg, U. (2016). Effect of Imperfect Interface on the Dynamic Response of a Circular Lined Tunnel Impacted by Plane P-Waves. *Tunn. Undergr. Space Technol.* 51, 68–74. doi:10.1016/j.tust.2015.10.011
- Yuan, Z., Cai, Y., Sun, H., Shi, L., and Pan, L. (2020). The Influence of a Neighboring Tunnel on the Critical Velocity of a Three-Dimensional Tunnel-Soil System [J]. *Int. J. Solids Struct.* 212, 23–45. doi:10.1016/j.ijsolstr.2020.11.026
- Zhang, P., Cai, J., Zong, F., He, Y., and Wang, Q. (2021). Dynamic Response Analysis of Underground Double-Line Tunnel under Surface Blasting. *Shock Vib.* 2021 (2), 1–13. doi:10.1155/2021/9226615
- Zhang, Z., Jia, J., Lu, S., and Dong, Q. (2022). Dynamic Response and Safety Criterion of Surrounding Rock of a Circular Tunnel Subjected to Cylindrical P-Waves [J]. *Arabian J. Geosciences* 15, 1–7. doi:10.1007/s12517-022-10091-9
- Zhou, Y., Wang, S. L., and Wang, J. (2016). Vibration Response of an Existing Tunnel to Adjacent Blasting Construction [J]. *Chem. Eng. Trans.* 55, 31–36. doi:10.1002/nag.2897
- Zlatanović, E., Šešov, V., Lukić, D. Č., and Bonić, Z. (2021). Influence of a New-bored Neighbouring Cavity on the Seismic Response of an Existing Tunnel under Incident P- and SV-waves. *Earthq. Engng Struct. Dyn.* 50 (11), 2980–3014. doi:10.1002/eqe.3497

Conflict of Interest: The authors declare that the research was conducted in the absence of any commercial or financial relationships that could be construed as a potential conflict of interest.

Publisher's Note: All claims expressed in this article are solely those of the authors and do not necessarily represent those of their affiliated organizations, or those of the publisher, the editors and the reviewers. Any product that may be evaluated in this article, or claim that may be made by its manufacturer, is not guaranteed or endorsed by the publisher.

Copyright © 2022 Lu, Yao, Jia, Sun, Ji and Zhang. This is an open-access article distributed under the terms of the Creative Commons Attribution License (CC BY). The use, distribution or reproduction in other forums is permitted, provided the original author(s) and the copyright owner(s) are credited and that the original publication in this journal is cited, in accordance with accepted academic practice. No use, distribution or reproduction is permitted which does not comply with these terms.